American Mineralogist, Volume 89, pages 307–313, 2004

Crystallographic properties of the calcium phosphate mineral, brushite, by means of First Principles calculations

C. IGNACIO SAINZ-DÍAZ,[1,*] ANA VILLACAMPA,[2] AND FERMÍN OTÁLORA[2]

[1] Estación Experimental del Zaidín, CSIC, C/ Profesor Albareda 1,18008-Granada, Spain,
[2] Laboratorio de Estudios Cristalográficos, IACT, CSIC-Universidad de Granada, Campus Fuentenueva s/n, 18002-Granada, Spain

ABSTRACT

A crystalline form of hydrated calcium phosphate, brushite ($CaHPO_4 \cdot 2H_2O$), has been studied by means of total energy First Principles calculations based on the Density Functional Theory (DFT) approximation. The experimental crystal lattice parameters of this mineral have been reproduced with good agreement. The powder X-ray diffraction pattern simulated from the calculated crystal structure is similar to the experimental one. The intermolecular interactions within the crystal, electrostatic and hydrogen bond interactions, have been reproduced. The calculated crystal structure reproduces the atomic distribution along the (010) surface observed by high resolution scanning force microscope (SFM). The optimized crystal structure describes the different interatomic interactions along the [101], [201], and [001] directions on the (010) plane. Quantum-mechanical calculations of the energy of these surfaces confirm the experimental behavior, justifying the different crystal growth rates of these directions found experimentally.

INTRODUCTION

Calcium phosphates are important biological minerals occurring in calcification processes (e.g., dentine, bone) and in pathological process (e.g., kidney stones, dental cavities). Brushite, calcium hydrogen phosphate dihydrate ($CaHPO_4 \cdot 2H_2O$), is formed in guano and phosphorite deposits, soils, and human calculi. It is a precursor to the formation of bones and teeth. Hence, its study is important for understanding biomineralization phenomena. It also has interesting industrial applications as an intermediate in phosphate fertilizer production and in pharmaceutical applications as a food additive and a component of tooth paste. Therefore, a study at the crystallographic level can be useful to help us understand some properties related to medical problems and industrial applications.

Crystals of brushite show a very variable morphology (Abbona et al. 1993). Single crystals are observed as well as twins and polycrystalline aggregates with more or less irregular crystals. As a mineral, it is found as a powder or an efflorescence of needle-like, prismatic, or tabular crystals. Most of the synthetic crystals are tabular. Some discrepancies appear in reports of the crystal structure. From its structural and morphological resemblance to the sulfur analogue gypsum and the arsenic analogue pharmacolite, it has been assumed for a long time to belong to the crystal class 2/*m* (Beevers 1958). All three analogues are compact correlated sheets, consisting of parallel chains of alternating anions and cations normal to the (010) plane, where calcium cations are coordinated by eight O atoms. However, Curry and Jones (1971) found that brushite has space group *Ia* belonging to the crystal class *m*. Several experimental studies have reported on the crystal growth and morphology of brushite (Abbona et al. 1993; Heijnen and Hartman 1991; Scudiero et al. 1999).

Many studies are being dedicated to the modeling of mineral structures at the atomic level, thanks to important advances in theory and computer technology in recent years (Lasaga 1995). Some studies with core-shell empirical models have reproduced some crystallographic and spectroscopic properties in silicates (Abbott 1991; Sainz-Díaz et al. 2001), however their transferability is limited. Calculations of hydrogen bonds in minerals with empirical models are not straightforward. The hydrogen bond interactions are important in the crystal structure and crystal growth of brushite, especially due to the presence of the hydrogen atom in the HPO_4 group and the water molecules included in the crystal lattice. Quantum mechanical studies have been applied on cluster models of silicates with interesting results (Lasaga 1995; Sainz-Díaz et al. 2000). First-principles quantum techniques, based on density functional theory (DFT) with periodic boundary conditions avoiding the edge effects associated with the cluster approach, have been used in the study of some minerals (e.g., Bridgeman et al. 1996; Sainz-Díaz et al. 2002; Sherman 1991; Smrcok and Benco 1996; Winkler et al. 2001).

Knowledge of the crystal growth mechanism is very important to understand biomineralization behavior. We propose in the present work the application of quantum mechanical methods to the study of the brushite crystal structure with two main aims: (1) to study the crystallographic properties of brushite by means of high-level theoretical methods and (2) to extend the application of First Principles methodology to minerals where hydrogen bonding is important.

METHODS

Total energy calculations based on DFT and pseudopotentials were performed with the CASTEP (Cambridge Serial Total Energy Package) software package and associated programs included in the Cerius2 graphical interface package (Payne et al. 1992). The electronic wavefunctions were expanded using a plane-wave basis set with an equivalent energy cut-off of 300 eV. Core electrons were replaced by ultra-soft pseudopotentials and gradient-corrected density functional theory was

*E-mail: sainz@eez.csic.es

used. The generalized gradient approximation (GGA) was used, because hydrogen-bonded systems are better described using gradient-corrected DFT (Lee et al. 1993). The Perdew-Burke-Ernzerhof parameterization of the exchange-correlation functional was employed (Perdew et al. 1996). The Monkhorst-Pack scheme (Monkhorst and Pack 1976) was used to sample the Brillouin zone. Two to eight **k**-points were used in the irreductible wedge of the Brillouin zone for both structures. In all of the structures, the atoms and cell parameters were relaxed controlling forces and the stress tensor by means of conjugated gradient minimizations.

The crystal surfaces were cleaved from the optimized crystal lattice, maintaining the same number of atoms in the crystal unit cell. A unit cell was built from this surface with a *c* cell parameter large enough to create a gap between the atoms of the different unit cells along the **c** axis (minimal distance 10.5–11.5 Å). The energy of this new unit cell was calculated with CASTEP using the same conditions. The surface energy is the difference between the energies of both unit cells per surface unit.

RESULTS

The experimental structural data were taken from the neutron diffraction and proton Nuclear Magnetic Resonance (^{1}H NMR) spectroscopy study of Curry and Jones (1971). They assigned the crystal to space group *Ia* which, unfortunately, is a non-standard group and is not listed in the International Tables. Thus, a change of space group was performed for the current study. Two groups of the International Tables are coherent with the symmetry of *Ia*; these are *Aa* and *Cc*. We choose *Cc* and the cell parameters and fractional coordinates of the atomic positions were transformed to the new space group following the standard procedure reported in http://lec.ugr.es/trans.

In Figure 1, the optimized crystal structure of brushite is presented, showing calcium phosphate groups (A) and water molecules (B) following a layer pattern of AABBAABB, as found previously by experiment (Curry and Jones 1971). The optimized structures reproduce the experimental values of lattice parameters (Table 1). Different optimizations were performed with several levels of energy cut-off (to 380 eV) and with several numbers of **k**-points (up to eight **k**-points), which yielded similar crystal structures. The calculated geometry is slightly closer to experimental results if an energy cut-off of 380 eV is used rather than 300 eV. This agreement was not increased by using higher values of the energy cut-off or more than two **k**-points. Good agreement was found between experimental and theoretical values of the bond lengths of the small molecules (water and phosphate) and in the O-Ca distances. The Ca cation is octa-coordinated with two O atoms of water molecules, five O atoms from phosphate O–P bonds, and the O atom of the O(H)–P bond of phosphate. All these Ca-O distances are similar, except the Ca···O(H)-P distance, which is clearly the highest value. The calculated values of these distances were very similar to the experimental ones with a standard deviation lower than 3% (Table 1). The O atoms are mostly tri-coordinated. Two O atoms of P-O groups are coordinated to two Ca cations each with strong electrostatic interactions [average O···Ca distance 2.45 (experiment)–2.50 (calculated) Å]. One of these O atoms has an additional coordination with a hydrogen atom of a water molecule [O···H distance of 2.79 (experiment)–2.81 (calculated) Å] and another O atom is coordinated to the H atom of the POH group (O···H distance of 1.64–1.69 Å). Another O atom of the P-O group is coordinated to one Ca (O···Ca distance of 2.58–2.62 Å) and two H atoms from water molecules (O···H distances of 1.78–1.81 Å). The O atom of the P-OH group is coordinated to

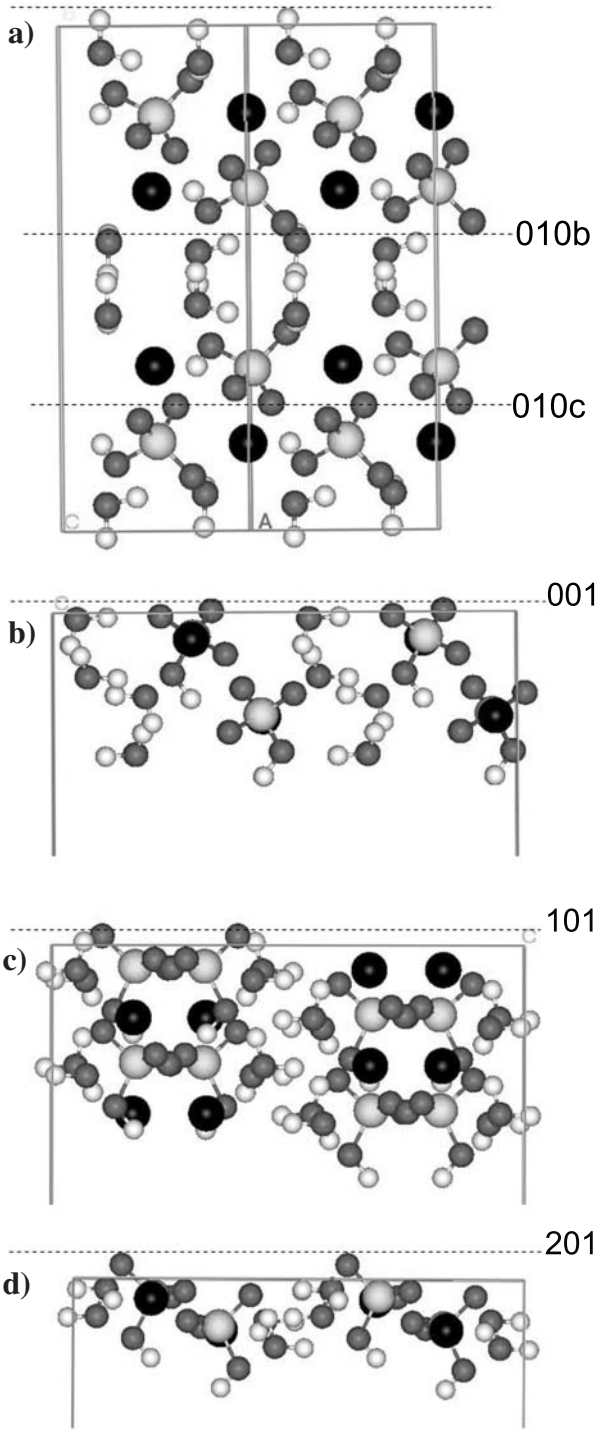

FIGURE 1. Crystal structure of brushite ($CaHPO_4 \cdot H_2O$); the Ca, P, O, and H atoms are represented by black, clear-gray, dark-gray, and white colors, respectively. The dashed lines represent the different possible terminations of the (010) surfaces (**a**), (001) (**b**), (101) (**c**), and (201) (**d**).

TABLE 1. Lattice parameters of the brushite structures (distances in angstroms and angles in degrees)

Parameters	Experimental *	Calculated	
		380 eV†	300 eV†
a	6.36	6.41	6.44
b	15.18	15.18	15.27
c	5.81	5.86	5.87
β	118.5	119.2	118.7
PO–H	1.000	1.015	1.016
P–O	(1.52)‡	(1.51)‡	
P–OH	1.61	1.59	
OH–H	(0.96)‡	(0.98)‡	(0.99)‡
Ca···OH2	2.38, 2.43 (2.41)‡	2.38, 2.46 (2.42)‡	2.41, 2.46 (2.44)‡
Ca···OHP	2.79	2.85	2.86
Ca···OP	2.35, 2.38, 2.48, 2.48, 2.58 (2.45)‡	2.37, 2.42, 2.50, 2.51, 2.62 (2.49)‡	2.38, 2.45, 2.52,2.53, 2.63(2.50)‡
PO–H···OP	1.69, 167.9	1.64, 168.1	1.62
PO–H···OH_2	2.79, 98.7	2.81, 96.8	
HO–H···OP	1.78, 1.81, 173.3	1.79, 1.73, 170.6	1.72, 1.84
P(H)O···H–OH	1.90, 167.4	1.87, 167.0	
HO–H···OH_2	2.16, 165.8	2.07, 164.8	

* From Curry and Jones (1971).
† Energy cut-off values.
‡ Averaged values in brackets.

TABLE 2. Fractional coordinates of the atomic positions (in angstroms) in the asymmetric unit for the experimental and optimized crystal structure of brushite

Atom*	Experimental†			Optimized‡		
	x	y	z	x	y	z
Ca	–0.506	0.327	0.250	–0.507	0.327	0.250
P	0.014	0.322	0.263	0.013	0.322	0.265
O1	–0.216	0.367	0.026	–0.211	0.367	0.026
O2	–0.080	0.282	0.434	–0.078	0.282	0.432
O3	0.202	0.393	0.393	0.199	0.393	0.397
O4	0.109	0.253	0.144	0.109	0.253	0.152
O5 (W)	–0.734	0.426	–0.111	–0.743	0.427	–0.119
O6 (W)	–0.274	0.447	0.508	–0.273	0.447	0.509
H1	–0.290	0.329	–0.133	–0.290	0.327	–0.134
H2 (W)	–0.748	0.490	–0.106	–0.750	0.492	–0.109
H3 (W)	–0.745	0.412	–0.281	–0.747	0.412	–0.288
H4 (W)	–0.279	0.509	0.499	–0.278	0.512	0.498
H5 (W)	–0.117	0.433	0.639	–0.110	0.432	0.645

* (W) = from water molecules.
† Based on the experimental cell parameters: a = 6.36, b = 15.18, c = 5.81 Å, β = 118.5°.
‡ Based on the calculated cell parameters with cut-off energy of 380 eV: a = 6.41, b = 15.18, c = 5.86 Å, β = 119.2°.

one Ca atom (O···Ca distance of 2.79–2.85 Å) and one H atom (O···H distance of 1.90–1.87 Å).

The intermolecular hydrogen bonding distances are also well reproduced by these calculations, the calculated values being slightly lower than the experimental ones. The strongest hydrogen bond is between the H atom of a POH group and the O atom of the PO group of another phosphate molecule with a H···O distance of 1.69 Å (experimental) and 1.64 Å (calculated), and an O-H···O angle of 167.9° (experimental) and 168.1° (calculated). This bond maintains the double layer of phosphate in the crystal structure. The water hydrogen atoms also form strong hydrogen bonds with the O atoms of the phosphate moiety (H···O distances of 1.78, 1.81, 1.90 Å, and O-H···O angles of 167.4–173.3°). However, the hydrogen bond between the H atom of the P-OH group and the water O atom is very weak with a long distance (2.79–2.81 Å) and a small angle (97–99°). The water molecules have weak hydrogen bonds to each other with a H···O distance of 2.16 Å.

Comparing the atomic positions of the experimental and optimized crystal structures, good agreement is observed for most atoms including the H atoms (Table 2). Slight differences are observed in the atoms of the water molecules, probably due to their higher mobility. Nevertheless, the average standard deviation is lower than 1% for all atoms. Radial distribution functions of the distances between different atoms were calculated for both theoretical and experimental structures. For the distances between the O and H atoms, similar patterns were observed for both structures yielding good agreement for the O-H bond lengths and long (O···H) distances, and slight differences for the strong hydrogen bonds (range of 1.6–2.2 Å) (Fig. 2). Similar patterns for the radial distribution function of the distances between the Ca and O atoms were found in the experimental and optimized structures (Fig. 3). The first coordination sphere of the Ca atom is well determined and no Ca-O values appear in the range 2.9–3.85 Å.

The simulated powder X-ray diffraction pattern based upon coordinates from the experimental data and the theoretical structures are in excellent agreement (Table 3) in terms of the peak positions and relative intensities of the main reflections. The diffraction pattern simulations were performed by using diffraction software implemented within the Cerius2 package with an X-ray wavelength of 1.54 Å. The range 5–45° 2θ was considered for comparison (Fig. 4). The experimental powder X-ray diffraction reflections (Sivakumar et al. 1998; Kumar et al. 1999) agree also with those of the calculated structure (Table 3), especially in terms of the peak positions. Small differences in the relative intensities were observed, although the two highest intensities correspond to the 020 and 021 reflections in all cases (Figs. 4a–d).

Observing the experimental and theoretical brushite crystal from the (010) plane, periodic rows of hydrogen-phosphate groups alternate with rows of calcium cations (Fig. 5). In the (010) surface, three directions are noted. These directions, [101], [201], and [001], correspond to the steps found experimentally by means of Scanning Force Microscopy (SFM) (Scudiero et al. 1999). We calculated the energy of the most significant surfaces at the quantum-mechanical level: (010), (001), (101), and (201) (Table 4). The (010) surface is clearly the most stable surface, as observed experimentally. Among the perpendicular planes with respect to the (010) surface, the relative energy follows the sequence: (201) > (101) > (001).

The (010) surface can present three possible molecular dispositions in the upper surface (Fig. 1): (1) one layer of water, (2) two layers of water, or (3) one layer of phosphate. All these possibilities were calculated and resulted in the following energy sequence: 1 < 2 < 3 (Table 4).

DISCUSSION

The asymmetry in the coordination of Ca by the phosphate groups can be seen in Figure 6. The Ca cation is coordinated to two water O atoms, two O atoms from different phosphate groups, and two O atoms from one phosphate group (Ph1). In the opposite direction, this Ca cation is also coordinated to other two O atoms from another phosphate group (Ph2) that forms a

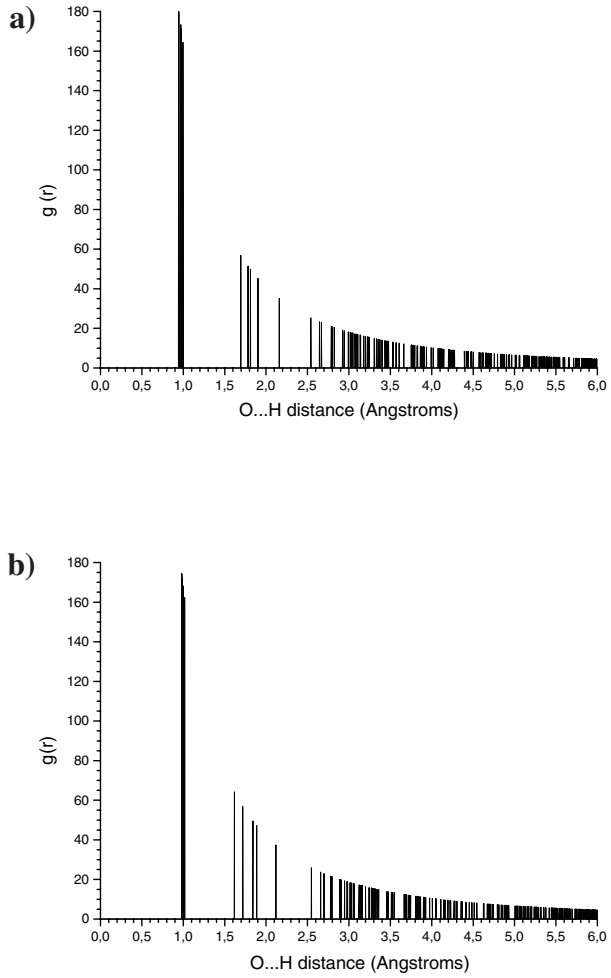

FIGURE 2. Radial distribution function of the O atoms and hydrogen atoms. Experimental geometry (**a**) and optimized structure (**b**).

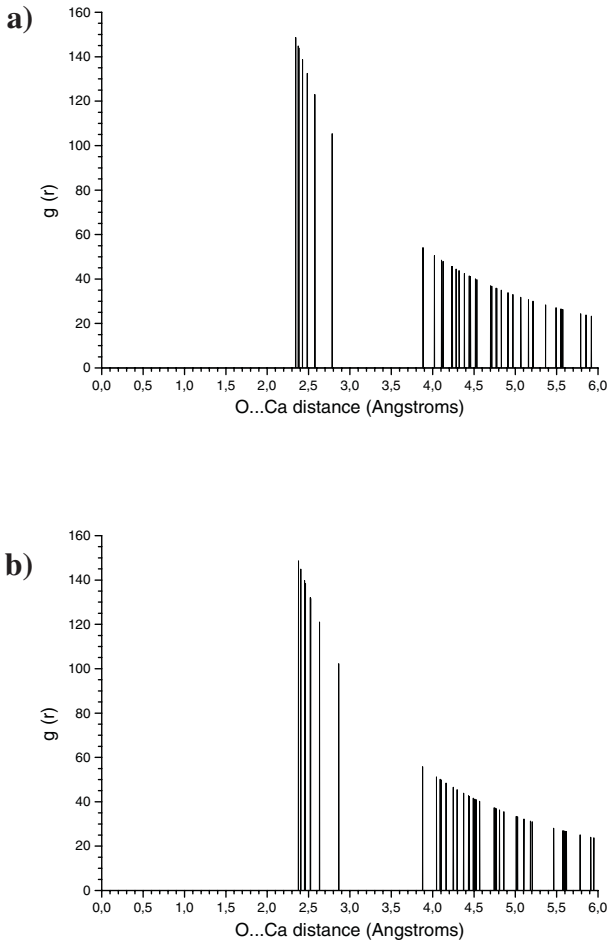

FIGURE 3. Radial distribution function of the calcium and O atoms. Experimental geometry (**a**) and optimized structure (**b**).

TABLE 3. Main reflections of the powder XRD patterns of the brushite structures

hkl	Exp.*		Exp.†		Optimized structure‡		Simulated§	
	2θ (°)	Int.#	2θ (°)	Int.#	2θ (°)	Int.#	2θ (°)	Int.#
020	11.8	82	11.4	68	11.6	100	11.6	100
021	20.8	100	20.8	100	20.9	92	20.9	90
04$\bar{1}$	29.1	82	29.2	61	29.3	73	29.3	70
22$\bar{1}$	30.3	66	30.3	15	30.3	51	30.5	46
15$\bar{1}$	33.9	78	34.0	18	34.1	63	34.2	50
022	36.7	30	36.9	14	36.8	15	36.9	16
15$\bar{1}$	40.9	26	40.0	19	39.8	4	39.8	4
24$\bar{2}$	41.5	24	41.5	11	41.7	29	41.6	19
221	44.4	17			44.4	3		

* Experimental data from Sivakumar et al. (1998).
† Experimental values (Kumar et al. 1999).
‡ Simulated from the crystal lattice calculated with 380 eV energy cut-off.
§ From single crystal experimental data (Curry and Jones 1971).
# Relative intensity (%).

perpendicular plane with respect to the O atoms of Ph1. However, the Ca···OP distances are different because the O atoms of Ph1 are O-P bonds [d(Ca···O) = 2.50 and 2.62 Å] and those from Ph2 group are O-P [d(Ca···O) = 2.50 Å] and O(H)-P [d(Ca···O) = 2.85 Å] bonds. This asymmetry has caused some confusion in the experimental structure determination in the past, and it is extended to the tri-coordinated O atoms.

Crystal structure is controlled by ionic interactions between the Ca cations and the O atoms from the phosphate groups and water molecules, and by hydrogen bond interactions between the phosphate groups, between the water and phosphate molecules, and between the water molecules themselves. The calculated structure corroborates the existence of two kinds of water molecules in brushite (Curry and Jones 1971). One water molecule is strongly bound by hydrogen bonds to phosphate O atoms, whereas in another water molecule the H atom interacts with the O atom of the former water molecule (Fig. 7).

TABLE 4. Calculated energies for the selected low-index surfaces of brushite using quantum-mechanical calculations

Surface*	Energy (J/m²)
(010)[1]	0.726
(010)[2]	1.209
(010)[3]	2.077
(001)	1.440
(101)	2.284
(201)	2.702

* In the (010) surface: 1 = one layer of water in the clean upper surface, 2 = two water layers in the upper surface, and 3 = one phosphate layer in the upper surface.

In brushite the average value of the P-O bond length is 1.52 Å (experiment) and 1.51 Å (calculated), and the P-OH bond length is 1.61 Å (experi-

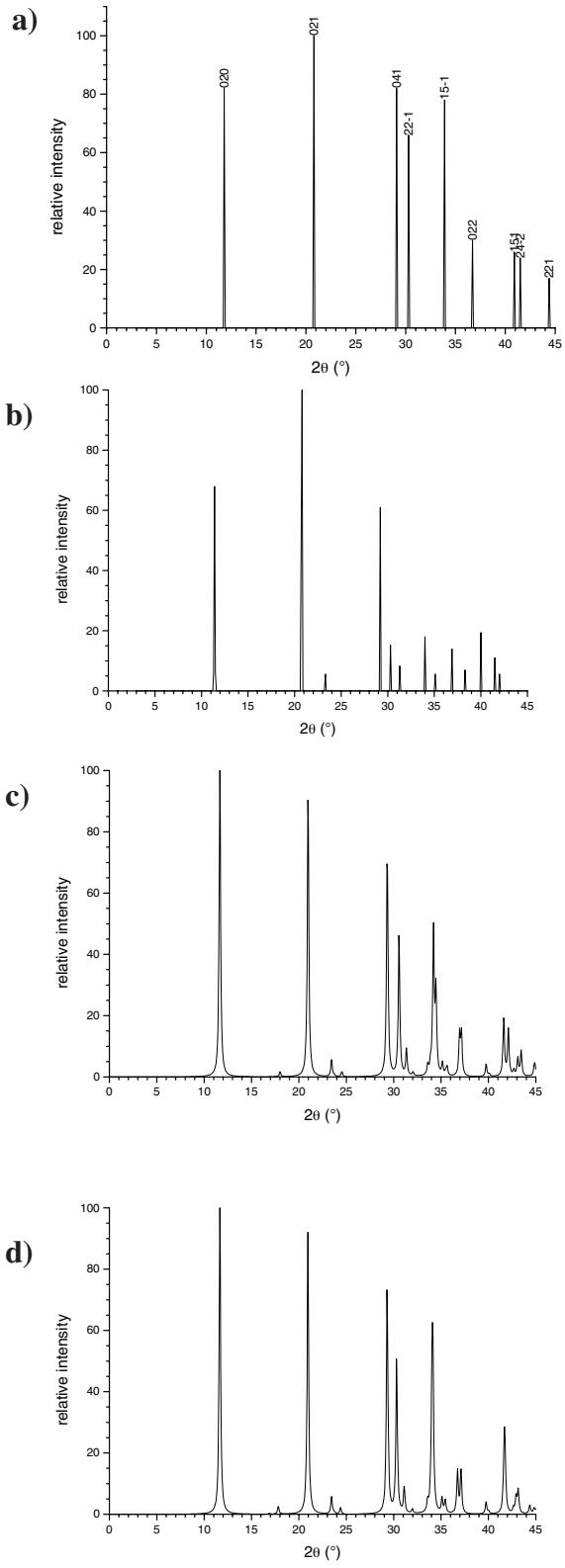

FIGURE 4. Powder X-ray diffraction patterns of brushite. Experimental data [Shivakumar et al. 1998 (**a**) and Kumar et al. 1999 (**b**)], simulated from the experimental single-crystal structure (**c**) and the theoretical crystal structure (**d**).

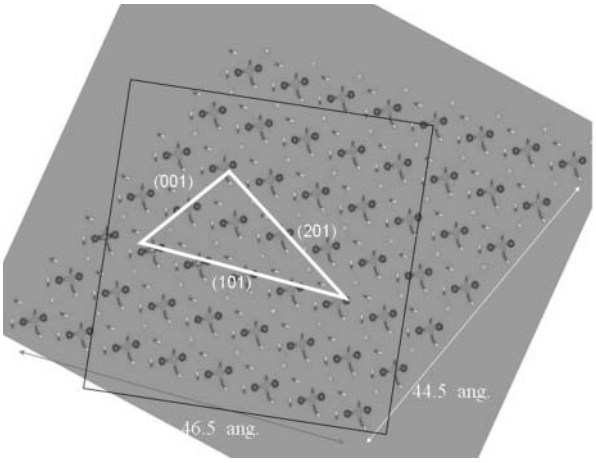

FIGURE 5. Atomic distribution in the calculated crystal structure of the (010) surface of brushite. The (101), (201), and (001) edges are highlighted.

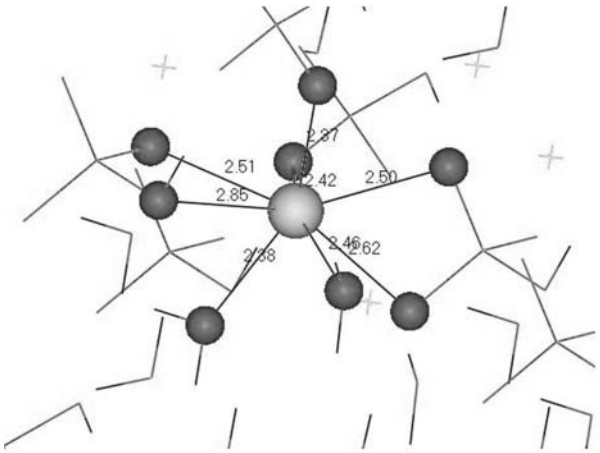

FIGURE 6. Coordination sphere of Ca in the calculated crystal lattice of brushite. The clear grey and dark grey balls represent Ca and O atoms, respectively. The main interatomic distances are included in angstroms.

ment) and 1.59 Å (calculated). In the anhydrous salt, monetite, a P-OH bond length of 1.59 Å has been reported (Curry and Jones 1971). A close relationship between the structure of the phosphate groups of brushite and some organophosphorides, such as alkenylphosphonic acids, can be observed. A P-OH bond length of 1.58 Å was found in crystals of vinylidene-bisphosphonic acid, where strong inter- and intra-molecular hydrogen bonding exist. Quantum mechanical calculations for this molecule yielded a P-OH bond length of 1.60 Å (Sainz-Díaz et al. 1995). These organophosphorides as well as the phosphate group have important properties of cation extractants due to their high facility of forming complexes (Sainz-Díaz et al. 1996). This property and the organic/inorganic-phosphate similarity can be very important for understanding some biomineralization processes, where brushite and phosphate groups are also implicated.

In crystal growth studies of brushite, the (010) plane is the most visible experimentally, meaning that it is the most stable surface. This fact was confirmed by means of our calculations.

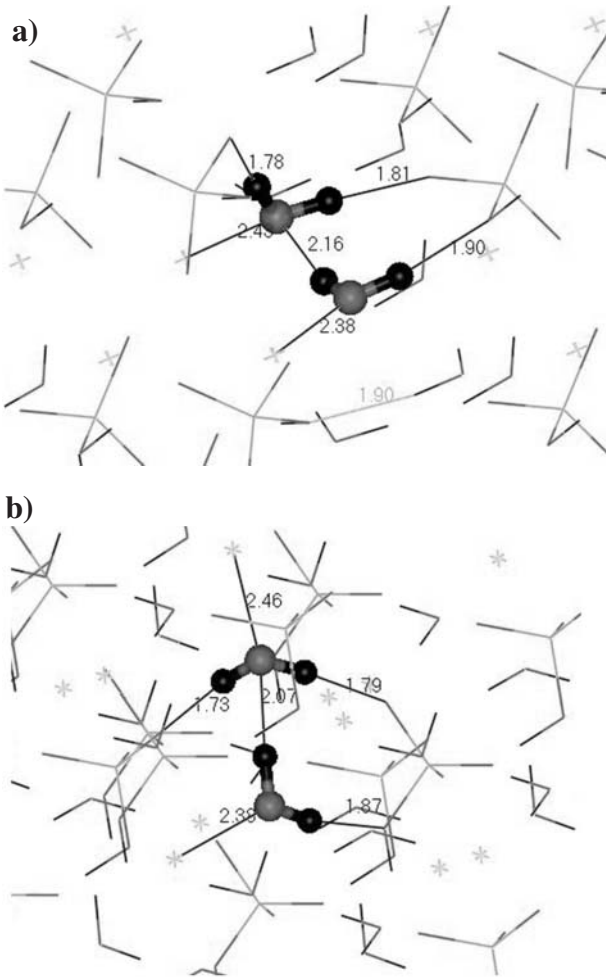

FIGURE 7. Structure and coordination of the water molecules in the brushite crystal lattice, experimental (**a**) and optimized (**b**) structures(different observation point in each case). The gray and black balls represent O and H atoms, respectively. The main interatomic distances are included in Å.

However, we have found three different possible terminations of this surface with different energies (Table 4). The termination with clean phosphate layers is highly energetic, it will be very unstable and it would attract water molecules in an aqueous medium. The most stable and probable termination of the (010) surface is that with only one layer of water. The (010) surface with two water layers has higher energy than that with only one water layer. This fact and the lack of water deposition on the highly energetic (010) surface with a clean phosphate layer lead us to consider the hypothesis of the existence of an aggregation unit formed by a hydrated complex of $[Ca(HPO_4{\cdot}2H_2O]_2$. This hypothesis is consistent with the high complexation capacity of the phosphate groups with cations (Sainz-Díaz et al. 1996) in comparison with sulfate or arsenate groups. Further experimental and theoretical investigations on the energetics, thermodynamics, and kinetics of the crystal growth process will yield more results to clarify this hypothesis.

This study considers three planes that are perpendicular to the (010) surface: (001), (101), and (201), taking into account the periodic bond chain (PBC) analysis of the morphology of brushite reported previously (Heijnen and Hartman 1991). These steps were also observed during corrosion studies of brushite by SFM. The dissolution rate follows a decrescent order of steps: (201) > (001) > (101). However, the rate for the (101) step is highly dependent on the stress, and the growth rate follows the sequence: (201) > (101) > (001) (Scudiero et al. 1999). Our calculations of the energy of these surfaces show the sequence: (201) > (101) > (001), consistent with the stability found experimentally for the (001), (101), and (201) steps. This result is also consistent with previous analysis of the bond strength density (BSD) of these steps where the values 0.067, 0.100, and 0.121 (bond/Å^2) were obtained for the (001), (101), and (201) steps, respectively (Scudiero et al. 1999). The lower the BSD, the higher the stability.

Our calculations reproduce the geometry of these steps, forming similar intersection angles to those observed experimentally. For example, the (201)/(101) angle is 32° (experimentally 31°, Scudiero et al. 1999). The calculated structure also reproduces the density of phosphate groups along each step observed by high resolution SFM (Scudiero et al. 1999).

The quantum-mechanical study presented in this work is a useful tool for reproducing the crystal structure of brushite and for analyzing the interatomic interactions and surface structures of this system. This fact is important to the extension of this methodology to the study of similar minerals and biogeochemical processes such as biomineralization, crystal growth, surface interactions, and crystal dissolution.

ACKNOWLEDGMENTS

This work was supported by DGES grant PPQ-2001-2932. The authors thank G.-R., K. Rosso, and two anonymous reviewers for their useful discussions, and the Centro Técnico de Informática of CSIC for computational support.

REFERENCES CITED

Abbona, F., Christensson, F., Franchini, A.M., and Lundager Madsen, H.E. (1993) Crystal habit and growth conditions of brushite, $CaHPO_4{\cdot}2H_2O$. Journal of Crystal Growth, 131, 331–346.

Abbott, R.N. Jr. (1991) A short range O-H potential for amphiboles based on OH stretching frequencies. Canadian Mineralogist, 29, 131–142.

Beevers, C.A. (1958) Crystal structure of brushite. Acta Crystallographica, 11, 273.

Bridgeman, C.H., Buckingham, A.D., Skipper, N.T., and Payne, M.C. (1996) Ab initio total energy study of uncharged 2:1 clays and their interaction with water. Molecular Physics, 89, 879–888.

Curry, N.A. and Jones, D.W. (1971) Crystal structure of brushite, calcium hydrogen orthophosphate dihydrate: a neutron-diffraction investigation. Journal of the Chemical Society A, 3725–3729.

Heijnen, W.M.M. and Hartman, P. (1991) Structural morphology of gypsum ($CaSO_4{\cdot}2H_2O$), brushite ($CaHPO_4{\cdot}2H_2O$) and pharmacolite ($CaHAsO_4{\cdot}2H_2O$). Journal of Crystal Growth, 108, 290–300.

Kumar, M., Xie, J., Chittar, K., and Riley, C. (1999) Transformation of modified brushite to hydroxyapatite in aqueous solution: effects of potassium substitution. Biomaterials, 20, 1389–1399.

Lasaga, A.C. (1995) Fundamental approaches in describing mineral dissolution and precipitation rates. In A.F. White and S.L. Brantley, Eds., Chemical Weathering Rates of Silicate Minerals, 31, 23–86. Reviews in Mineralogy, Mineralogical Society of America, Washington, D.C.

Lee, C., Vanderbilt, D., Laasonen, K., Car, R., and Parrinello, M. (1993) Ab initio studies on the structural and dynamical properties of ice. Physical Review B, 47, 4863–4872.

Monkhorst, H.J. and Pack, J.D. (1976) Special points for Brillouin-zone integration. Physical Reviews B, 13, 5188–5192.

Payne, M.C., Teter, M.P., Allan, D.C., Arias, T.A., and Joannopoulos, J.D. (1992) Iterative minimization techniques for ab initio total-energy calculations: molecular dynamics and conjugate gradients. Reviews in Modern Physics,

64, 1045–1097.
Perdew, J.P., Burke, K., and Ernzerhof, M. (1996) Generalized gradient approximation made simple. Physical Review Letters, 77, 3865–3868.
Sainz-Díaz, C.I., Hernández-Laguna, A., Smeyers, N.J., and Smeyers, Y.G. (1995) An ab initio comparative structural study of alkenylphosphonic acid derivatives. Journal of Molecular Structure, 330, 231–242.
Sainz-Díaz, C.I., Klocker, H., Marr, R., and Bart, H.-J. (1996) New approach in the modelling of the extraction equilibrium of zinc with bis-2-ethylhexylphosphoric acid. Hydrometallurgy, 42, 1–11.
Sainz-Díaz, C.I., Timón, V., Botella, V., and Hernández-Laguna, A. (2000) Isomorphous substitution effect on the vibration frequencies of hydroxyl groups in molecular cluster models of the clay octahedral sheet. American Mineralogist, 85, 1038–1045.
Sainz-Díaz, C.I., Hernández-Laguna, A., and Dove, M.T. (2001) Modelling of dioctahedral 2:1 phyllosilicates by means of transferable empirical potentials. Physics and Chemistry of Minerals, 28, 130–141.
Sainz-Díaz, C.I., Timón, V., Botella, V., Artacho, E., and Hernández-Laguna, A. (2002). Quantum mechanical calculations of dioctahedral 2:1 phyllosilicates. Effect of octahedral cation distributions in pyrophyllite, illite and smectite. American Mineralogist, 87, 958–965.
Scudiero, L., Langford, S.C., and Dickinson, J.T. (1999). Scanning force microscope observations of corrosive wear on single-crystal brushite ($CaHPO_4 \cdot 2H_2O$) in aqueous solution. Tribology Letters, 6, 41–55.
Sherman, D.M. (1991) Hartree-Fock band structure, equation of state, and pressure-induced hydrogen bonding in brucite, $Mg(OH)_2$. American Mineralogist, 76, 1769–1772.
Sivakumar, G.R., Girija, E.K., Kalkura, S.N., and Subramanian, C. (1998) Crystallization and characterization of calcium phosphates: brushite and monetite. Crystallization Research Technology, 33, 197–205.
Smrcok, L. and Benco, L. (1996) Ab initio periodic Hartree-Fock study of lizardite 1T. American Mineralogist, 81, 1405–1412.
Winkler, B., Milman, V., Hytha, M., Pickard, C.J., and Warren, M. (2001) Theoretical investigation of bonding in diaspore. European Journal of Mineralogy, 13, 343–349.

MANUSCRIPT RECEIVED JANUARY 29, 2003
MANUSCRIPT ACCEPTED JULY 7, 2003
MANUSCRIPT HANDLED BY KEVIN ROSSO